Inorg. Chem. **2008**, *47*, 6106−6108

Cyanide-Bridged Iron(II,III) Cube with Multistepped Redox Behavior

Masayuki Nihei, Mayumi Ui, Norihisa Hoshino, and Hiroki Oshio*

Graduate School of Pure and Applied Sciences, Department of Chemistry, University of Tsukuba, Tennodai 1-1-1, Tsukuba 305-8571, Japan

Received December 20, 2007

A building unit of Prussian blue was isolated as a cyanide-bridged iron cube of $[Fe^{II}_4Fe^{III}_4(CN)_{12}(tp)_8]\cdot 12DMF\cdot 2Et_2O\cdot 4H_2O$ [tp^- = hydrotris(pyrazolyl)borate]. A cyclic voltammogram showed quasi-reversible four-stepped redox waves, which correspond to $[Fe^{III}_4Fe^{II}_4]/[Fe^{III}_5Fe^{II}_3]^+$, $[Fe^{III}_5Fe^{II}_3]^+/[Fe^{III}_6Fe^{II}_2]^{2+}$, $[Fe^{III}_6Fe^{II}_2]^{2+}/[Fe^{III}_7Fe^{II}_1]^{3+}$, and $[Fe^{III}_7Fe^{II}_1]^{3+}/[Fe^{III}_8]^{4+}$ processes. Controlled potential absorption spectral measurements revealed two intervalence charge-transfer bands at 816 and 1000 nm, which were assigned to charge transfers from Fe^{II} ions to adjacent and remote Fe^{III} ions, respectively, in the cube.

A cyanide ion is a useful bridging ligand to construct discrete molecules and 1D−3D architecture, and they have garnered intense research interest because of their solid-state properties. Prussian blue and some analogues exhibit magnetic ordering with Curie temperatures ranging from 5 K to room temperature,[1] while some discrete molecules show superparamagnetism[2] and spin-state conversion with external stimuli.[3] Among cyanometalates with different sizes, octanuclear complexes with a cubic structure, formulated as $[M_4M'_4(\mu\text{-}CN)_{12}]^{n+}$, are challenging target molecules because they are the smallest building units of Prussian blue analogues.[4] We report here the first cyanide-bridged iron cube, $[Fe^{II}_4Fe^{III}_4(\mu\text{-}CN)_{12}(tp)_8]\cdot 12DMF\cdot 2Et_2O\cdot 4H_2O$ [**1**; tp^- = hydrotris(pyrazolyl)borate], and its mixed-valence properties were characterized.

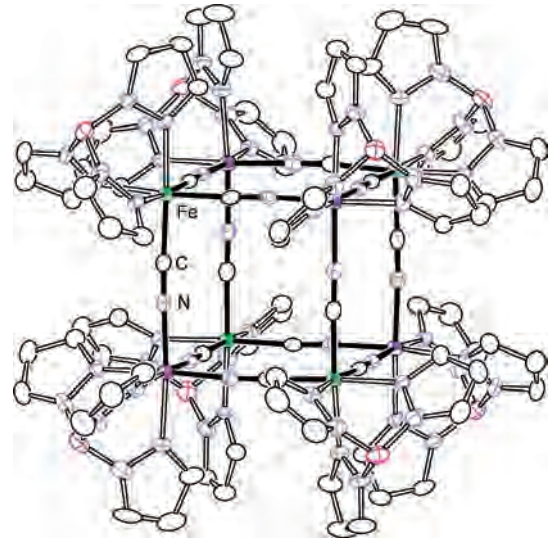

Figure 1. ORTEP diagram of **1** with 30% probability.

The reaction of $(Bu_4N)[Fe(CN)_3(tp)]$[5] with $Fe(OTf)_2\cdot 4H_2O$ and K(tp) yielded the octanuclear complex **1** as green cubic crystals.[6] **1** crystallizes in monoclinic space group $P2_1/c$, and the molecule lies on a center of symmetry. The complex has eight iron ions that are bridged by cyanide, and the overall core structure is nearly cubic (Figure 1). Charge considerations, Mössbauer spectroscopic measurements (Figure 2), and magnetic data (Figure S3 in the Supporting Information) suggest that **1** has four low-spin (LS) Fe^{II} and four high-spin (HS) Fe^{III} ions. ^{57}Fe Mössbauer spectra of **1** at 20, 200, and 293 K were nearly identical and mainly composed of two doublets (Figure 2 and Figure S2 in the Supporting

* To whom corresponding author should be addressed. E-mail: oshio@chem.tsukuba.ac.jp.

(1) (a) Holden, A. N.; Matthias, B. T.; Anderson, P. W.; Lewis, H. W. *Phys. Rev.* **1956**, *102*, 1463. (b) Ferlay, S.; Mallah, T.; Ouahès, R.; Veillet, P.; Verdaguer, M. *Nature* **1995**, *378*, 701. (c) Sato, O.; Iyoda, T.; Fujishima, A.; Hashimoto, K. *Science* **1996**, *271*, 49. (d) Miller, J. S. *MRS Bull.* **2000**, *25*, 60.

(2) (a) Sokol, J. J.; Hee, A. G.; Long, J. R. *J. Am. Chem. Soc.* **2002**, *124*, 7656. (b) Choi, H. J.; Sokol, J. J.; Long, J. R. *Inorg. Chem.* **2004**, *43*, 1606. (c) Schelter, E. J.; Karadas, F.; Avendano, C.; Prosvirin, A. V.; Wernsdorfer, W.; Dunbar, K. R. *J. Am. Chem. Soc.* **2007**, *129*, 8139.

(3) (a) Herrera, J. M.; Marvaud, V.; Verdaguer, M.; Marrot, J.; Kalisz, M.; Mathonière, C. *Angew. Chem., Int. Ed.* **2004**, *43*, 5468. (b) Nihei, M.; Ui, M.; Yokota, M.; Han, L.-Q.; Maeda, A.; Kishida, H.; Okamoto, H.; Oshio, H. *Angew. Chem., Int. Ed.* **2005**, *44*, 6484.

(4) (a) Li, D.; Parkin, S.; Wang, G.; Yee, G. T.; Clérac, R.; Wernsdorfer, W.; Holmes, S. M. *J. Am. Chem. Soc.* **2006**, *128*, 4214. (b) Yang, J. Y.; Shores, M. P.; Sokol, J. J.; Long, J. R. *Inorg. Chem.* **2003**, *42*, 1403. (c) Schelter, E. J.; Prosvirin, A. V.; Dunbar, K. R. *J. Am. Chem. Soc.* **2004**, *126*, 15004. (d) Kim, J.; Han, S.; Lim, J. M.; Choi, K.-Y.; Nojiri, H.; Suh, B. J. *Inorg. Chim. Acta* **2007**, *360*, 2647.

(5) Kim, J.; Han, S.; Cho, I.-K.; Choi, K. Y.; Heu, M.; Yoon, S.; Suh, B. J. *Polyhedron* **2004**, *23*, 1333.

(6) $[Fe^{II}_4Fe^{III}_4(m\text{-}CN)_{12}(tp)_8]\cdot 12DMF\cdot 2Et_2O\cdot 4H_2O$ (**1**): $C_{128}H_{192}N_{72}B_8Fe_8O_{18}$, M = 3560.67, monoclinic, $P2_1/c$, a = 17.983(4) Å, b = 32.249(7) Å, c = 17.424(4) Å, b = 109.347(4)°, V = 9534(4) Å^3, Z = 2, T = 200 K, r_{calcd} = 1.240 g/cm^3, μ = 0.664 mm^{-1}, $F(000)$ = 3703, 41 870 reflections collected, λ = 0.710 73 Å, 1081 parameters for 13 688 independent reflections with $I > 2\sigma$ gave R1 = 0.0764 and wR2 = 0.2165. Anal. Calcd for $C_{84}H_{80}N_{60}B_8Fe_8\cdot 4DMF\cdot 3H_2O$ (dried sample): C, 41.04; H, 4.09; N, 31.91. Found: C, 40.90; H, 4.06; N, 31.72.

10.1021/ic7024582 CCC: $40.75
Published on Web 06/19/2008

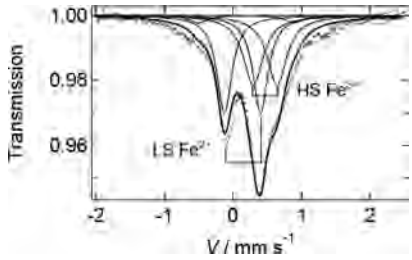

Figure 2. Mössbauer spectrum of **1** at 20 K.

Information).[7] Their Mössbauer parameters were $\delta = 0.14$ and $\Delta E_Q = 0.53$ mm s^{-1} and $\delta = 0.47$ and $\Delta E_Q = 0.35$ mm s^{-1} at 20 K, characteristic of LS Fe^{II} and HS Fe^{III} species, respectively. An additional small doublet with $\delta = 0.19$ and $\Delta E_Q = 1.39$ mm s^{-1} is due to a paramagnetic impurity of LS Fe^{III} species. The peak area ratio (0.50/0.47) of the two main peaks suggested a 1:1 ratio of LS Fe^{II} and HS Fe^{III} ions. Cyanide carbon atoms act as π acceptors and cause a stronger ligand field on the metal ions, and this stabilizes LS states.[8] It is, therefore, considered that the cyanide carbon and nitrogen atoms coordinate to LS Fe^{II} and HS Fe^{III} ions, respectively. Note that **1** was prepared by using $[Fe(CN)_3(tp)]^-$ as a starting material, in which the cyanide carbon atoms coordinate to Fe^{III} ions. Electron transfers from $[(tp)Fe(CN)_3]^{1-}$ to $[(tp)Fe^{II}]^{1+}$ sites are suggested to occur during the reaction, leading to a Fe^{II}−CN−Fe^{III} oxidation state.[9] Additional support for the bridging mode was found in an IR spectrum of **1** (Figure S1 in the Supporting Information). In the IR spectrum, **1** exhibited three peaks at 2098, 2079, and 2057 cm^{-1}, which can be assigned to ν_{CN} stretches characteristic of M^{II}−CN−M^{III} bridges.[9,10]

X-ray structure analyses showed that the cube locates on the inversion center and consists of four crystallographically independent iron ions. The iron ions on the opposite sites in the cube should be crystallographically identical; however, the alternate arrangement of LS Fe^{II} and HS Fe^{III} moieties in the cube implies that the iron ions on the opposite corners are not equivalent to each other. It is considered that positional disorders of the cubes exist in the crystals.[4d] As a result, the iron ions in the cube exhibit a distorted octahedral coordination geometry with similar coordination bond lengths. Note that structural analysis with a nonsymmetric space group did not give satisfactory results. Cyanide carbon and nitrogen atoms were, therefore, treated as the atoms with 0.5C/0.5N in the X-ray structural analyses. Facial coordination sites of the iron ions are occupied by three nitrogen atoms from tp$^-$, and the remaining sites are coordinated by either carbon or nitrogen atoms of the cyanide groups. Coordination bond lengths are in the range of 1.945(6)−1.958(7) Å for Fe−C_{CN} or Fe−N_{CN} bonds and in the range of 2.062(5)−2.085(5) Å for Fe−N_{tp} bonds. Vertex angles of the cube are close to right angles [91.1(2)−93.2(2)°], and the Fe^{II}−C−N and Fe^{III}−N−C angles on the sides of the cube are nearly linear [175.3(5)−179.6(6)°].

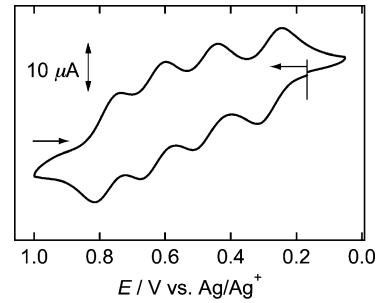

Figure 3. Cyclic voltammogram of **1** (potential vs Ag/Ag$^+$, 1 mM, 0.1 M Bu_4NPF_6 in CH_2Cl_2, glassy carbon working electrode, Pt wire counter electrode, and a scan rate of 50 mV s^{-1} at 20 °C).

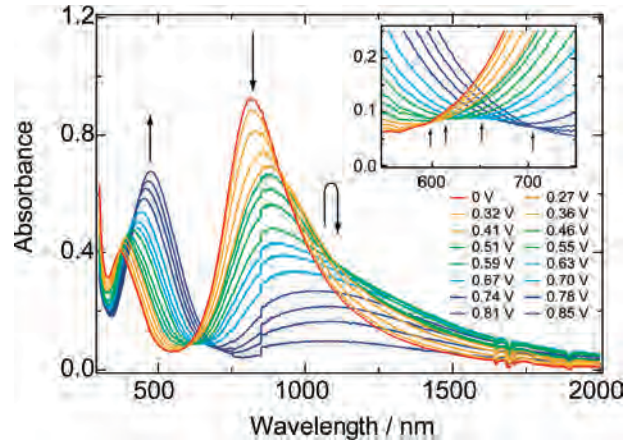

Figure 4. Electronic absorption spectra of **1** upon electrochemical oxidation from 0 to 0.85 V (potential vs Ag/Ag$^+$, 0.6 mM, 0.1 M Bu_4NPF_6 in CH_2Cl_2, Pt mesh working electrode, and Pt wire counter electrode). Arrows represent absorbance changes upon electrochemical oxidation.

A cyclic voltammogram (Figure 3) of **1** showed four quasi-reversible redox waves at 0.28, 0.48, 0.64, and 0.78 V (vs Ag/Ag$^+$), and they were assigned to four one-electron redox processes of $[Fe^{III}_4Fe^{II}_4]/[Fe^{III}_5Fe^{II}_3]^+$, $[Fe^{III}_5Fe^{II}_3]^+/[Fe^{III}_6Fe^{II}_2]^{2+}$, $[Fe^{III}_6Fe^{II}_2]^{2+}/[Fe^{III}_7Fe^{II}_1]^{3+}$, and $[Fe^{III}_7Fe^{II}_1]^{3+}/[Fe^{III}_8]^{4+}$, respectively. The first redox potential of **1** is close to that ($E_{1/2}$ = 0.27 V) of the mononuclear complex, $[Fe^{II}(CN)_2(bpy)_2]$,[11] suggesting that the cyanide carbon atoms coordinate to the LS Fe^{II} ions in **1**. The redox potential difference (ΔE) is a measure of the stability of mixed-valence states, and they are generally represented by comproportionation constants (K_c).[12] ΔE values of 0.20, 0.16, and 0.14 V for the four redox waves yielded K_c values of 2.7×10^3, 5.6×10^2, and 2.5×10^2 for $[Fe^{III}_5Fe^{II}_3]^+$, $[Fe^{III}_6Fe^{II}_2]^{2+}$, and $[Fe^{III}_7Fe^{II}_1]^{3+}$, respectively, indicating an intermediate thermodynamic stability of the mixed-valence states (class II).

Controlled potential absorption spectra of **1** in CH_2Cl_2 were measured by applying potentials in the range of 0 −0.85 V (vs Ag/Ag$^+$; Figure 4). Before oxidation, the absorption spectrum (the red curve in Figure 4) was mainly composed of peaks at 370 and 816 nm and a ligand-based band was

(7) Mössbauer parameters are calculated relative to the metal iron.
(8) Vahrenkamp, H.; Geib, A.; Richardson, G. N. *J. Chem. Soc., Dalton Trans.* **1997**, 3643.
(9) Li, D.; Clérac, R.; Roubeau, O.; Harté, E.; Mathoniére, C.; Bris, R. L.; Holmes, S. M. *J. Am. Chem. Soc.* **2008**, *130*, 252.
(10) Shatruk, M.; Dragulescu-Andrasi, A.; Chambers, K. E.; Stoian, S. A.; Bominaar, E. L.; Achim, C.; Dunbar, K. R. *J. Am. Chem. Soc.* **2007**, *129*, 6104.
(11) (a) Oshio, H.; Onodera, H.; Tamada, O.; Mizutani, H.; Hikichi, T.; Ito, T. *Chem.—Eur. J.* **2000**, *6*, 2523. (b) Oshio, H.; Onodera, H.; Ito, T. *Chem.—Eur. J.* **2003**, *9*, 3946.
(12) $K_c = \exp(F\Delta E/RT)$.

observed in the UV region. The band at 370 nm, which was analyzed by two Gaussian peaks with peak maxima at 357 and 417 nm, moves to the lower energy region (475 nm), and these bands were tentatively assigned to a metal-to-ligand (ML) or ligand-to-metal (LM) charge-transfer (CT) process. Note that MLCT and LMCT bands were observed at 337−425 nm for $[Fe^{II}(tp)_2]$, $[Fe^{II}(CN)_3(tp^*)]^{2-}$, and $[Fe^{III}(CN)_3(tp^*)]^-$ [tp* = hydrotris(dimethylpyrazolyl)borate].[13] Upon electrochemical oxidation, the band absorbance at 816 nm decreased steadily and red-shifted and a new band appeared around 1000 nm. Note that four isobestic points were observed at 597, 617, 650, and 700 nm upon electrochemical oxidation, corresponding to the four $1e^-$ oxidations from $[Fe^{III}_4Fe^{II}_4]$ to $[Fe^{III}_8]^{4+}$ (Figure 4. inset). Band assignments of the peaks at 816 and 1000 nm were not straightforward. There are two intervalence charge-transfer (IVCT) transitions in **1**, that is, between adjacent iron ions ($Fe^{II}-CN-Fe^{III}$) and between remote iron ions ($Fe^{II}-CN-Fe^{III}-NC-Fe^{III}$), called *adjacent* and *remote* IVCT transitions, respectively. $KFe^{III}[Fe^{II}(CN)_6]$ shows an IVCT band around 700 nm,[14] and, thus, the band at 816 nm in **1** was assigned to be the *adjacent* IVCT band. A *remote* IVCT originates from a symmetric mixed-valence state, which results in a lower energy than that for the *adjacent* IVCT band.[15] The band around 1000 nm was, therefore, assigned to be the *remote* IVCT band. Note that the initial decrease of the *adjacent* IVCT band is coupled to an increase in the *remote* IVCT band before the absorbance in both bands tends to zero, as the fully oxidized $[Fe^{III}_8]^{4+}$ state is reached. This is due to the decrease in the number of Fe^{II} ions in **1**. Magnetic susceptibility measurements for **1** were performed in the temperature range of 4.0−300 K (Figure S3 in the Supporting Information), and the Curie plot gave a straight line with $C = 16.85$ emu mol^{-1} K and $\theta = -1.17$ K. The Curie constant corresponds to the calculated value for the four noncorrelated HS Fe^{III} ions. The weak antiferromagnetic interactions between HS Fe^{III} ions are operative in the cube (Figure S4 in the Supporting Information).

Acknowledgment. This work was supported by a Grant-in-Aid for Scientific Research from the Ministry of Education, Science, Sports and Culture, Japan.

Supporting Information Available: Synthesis, characterization, physical measurements, IR spectrum, Mössbauer spectra, magnetic susceptibility data, and crystallographic details in CIF format. This material is available free of charge via the Internet at http://pub.acs.org.

IC7024582

(13) (a) Li, D.; Parkin, S.; Wang, G.; Yee, G. T.; Holmes, S. M. *Inorg. Chem.* **2006**, *45*, 1951. (b) Jesson, J. P.; Trofimenko, S.; Eaton, D. R. *J. Am. Chem. Soc.* **1967**, *89*, 3158.

(14) Robin, M. B. *Inorg. Chem.* **1962**, *1*, 337.

(15) (a) D'Alessandro, D. M.; Keene, F. R. *Chem. Rev.* **2006**, *106*, 2270. (b) Roffia, S.; Paradisi, C.; Bignozzi, C. A. *J. Electroanal. Chem.* **1986**, *200*, 105.